

## Design And Fabrication Flow Focusing Microfluidic Device For Continuous Dielectrophoretic Separation

Naqib Fuad Abd Rashid<sup>1</sup>, Azrul Azlan Hamzah<sup>1</sup>, M. F. Mohd Razip Wee<sup>1</sup> and Muhamad Ramdzan Buyong<sup>1\*</sup>

<sup>1</sup>*Institute of Microengineering and Nanoelectronics (IMEN), Universiti Kebangsaan Malaysia (UKM).*

### ABSTRACT

*We present a flow focusing microfluidic device for continuous dielectrophoretic separation. Our method relies on our unique microfluidic geometry which performs hydrodynamic focusing, generates flow with three inlets and three outlets. To improve particle separation in array type microelectrode, we hydrodynamically focus the main flow into the region of interest to the gap between the two electrodes. We design the geometry of the device using 3D CAD software and study the fluid flow using Comsol Multiphysics 5.4. Then, we fabricate this microfluidics device using the micro-milling process combine with soft lithography using PDMS. Lastly, we do an experimental flow setup using our microfluidic device to see the hydrodynamic flow focusing within the channel with three different main flow rate ratio to the sheath flow.*

**Keywords:** Flow Focusing, Microfluidic, Dielectrophoresis, Microfluidics Fabrication, Flow Simulation, Lab On Chip.

### 1. INTRODUCTION

Some biomedical analyses are performed based on specific kinds of cell presents from a body sample. Accomplishment in such analyses relies upon the capacity to manipulate and isolate the particles from its main sample. In conventional methods, there a lot of steps and equipment needed to manipulate and isolate the particles such as centrifuges, magnets, and macroscale filters. This step is very time consuming and high cost. Microfluidics, the science of fluid manipulation at a microscale level, has been grown exponentially to bridge this gap. At this scale, researchers can exploit the scaling of numerous physical laws and utilize, for instance, laminar flow [1], dean flow [2], rapid diffusion [3], rapid thermal transport [4] and exploit the large surface area relative to the volume [5]. These varied advantages have helped microfluidics discover applications in numerous fields, including biomedical separation applications. The process used for manipulation and isolation of the cells and particles in microfluidics already been scaled down and required a small number of samples. Differences in the biological and physical properties of the targeted cells are the way into the improvement of these techniques. In microfluidics, particle manipulation can be classified into active and passive techniques [6]. The active technique utilized external fields such as electrical, magnetic, acoustic, and optical to drive-cells for separation, while the passive technique utilized channel structure and intrinsic hydrodynamic forces to manipulate cells [7]. Here we focus on creating a microfluidic device that involved a combination of flow focusing and continuous dielectrophoresis force.

Dielectrophoresis (DEP) refers to the motion of polarizable particles suspended in a fluid flow, induced by a spatially non-uniform electrical field [8]. Particles that are more polarizable than the suspended medium will move towards the region of the strong electrical field, and such a movement is called positive dielectrophoresis (pDEP) [9] while the particles that are less

---

\*Corresponding Author: [muhdrmdzan@ukm.edu.my](mailto:muhdrmdzan@ukm.edu.my)

polarizable than the suspended medium will move towards a low electrical field. This motion is referred to as negative dielectrophoresis (nDEP) [10].

Generally, in the array type microelectrodes, the region of the high electrical field is situated at the edges between two microelectrodes [11], as in Figure 1. The effectiveness of the DEP force in the array type electrodes also can be seen in the Finite Element Method (FEM) studies done by Buyong *et al.*, where the DEP force is dominant within this region [12]. Therefore, in this region, the DEP force is higher compared to other regions and strong enough to influence the movement of particles in a continuous flow. While in the other region, fluid-particles interaction will be dominant by a drag force, and to isolate and manipulate the particles will be hard. Thus, to have an optimum separation and isolate targeted particles, the particles in a continuous flow need to be in the region of interest (ROI).

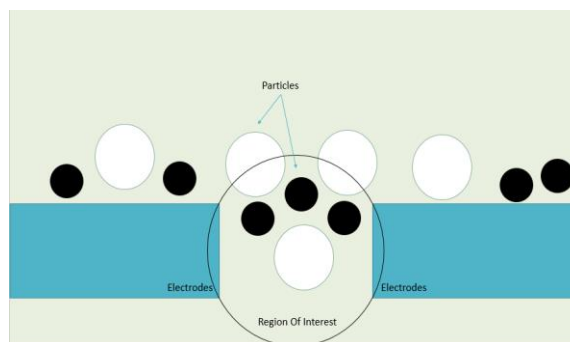


**Figure 1.** ROI between two electrodes in array type microelectrode.

In microfluidics, fluid flow within its channels is laminar since it is typically characterized by low Reynolds numbers. The numerator of the Reynolds number is very small due to the channels having dimensions ranging from nanometers to millimetres, while the denominator, viscosity, remains constant for most fluids. So in the laminar flow region, the fluid flow is characterized by parallel lines flowing linearly with no mixing occurs and is seen as very orderly flow. This phenomenon can be used in the hydrodynamic focusing technique. Hydrodynamic focusing technique is a technique by introducing sheath fluid from the side of the main flow to squeeze the flow sample [13]. So a flow focusing is created because the sample fluid will not mix with the sheath fluid under the laminar region. As can be seen in Figure 2, the sample flow,  $Q_C$ , is focused and sheathed downstream by sheath flow  $Q_B$  and  $Q_A$ . By utilizing this phenomenon in microfluidics, we can focus the targeted particles into the region of interest and improve DEP efficiency in array type microelectrode.

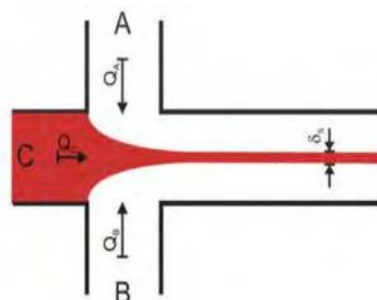


**Figure 2.** Hydrodynamic Flow Focusing.

For normal microfluidic devices, the particles in the flow are dispersed within the flow. Thus the particles are not situated in the ROI. While for flow focusing microfluidic devices, the particles are focused on the ROI. So all the particles will experience a greater DEP force. Figure 3 (a) and (b) show the differences in particles flow in both situations.

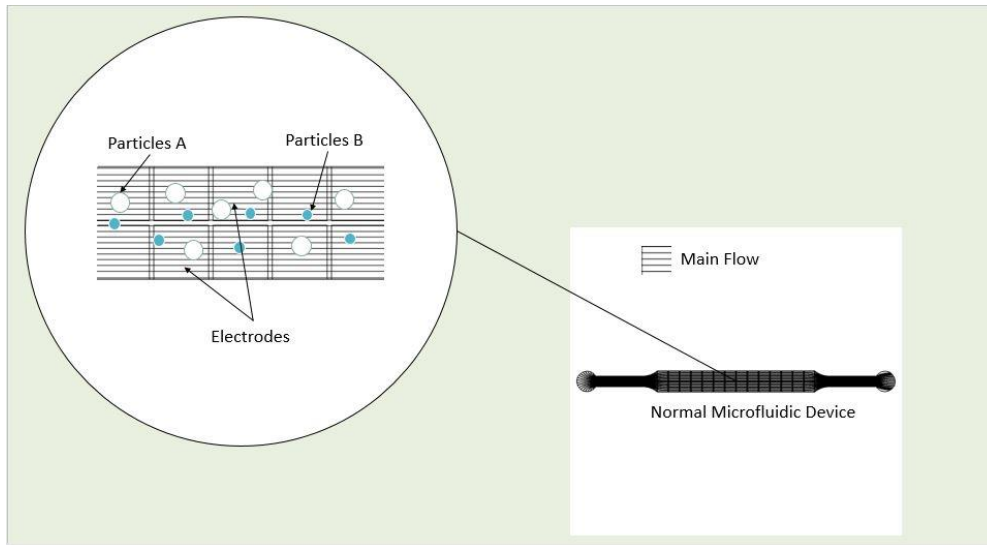


**Figure 3 (a).** Particles flow in normal Microfluidic Device.

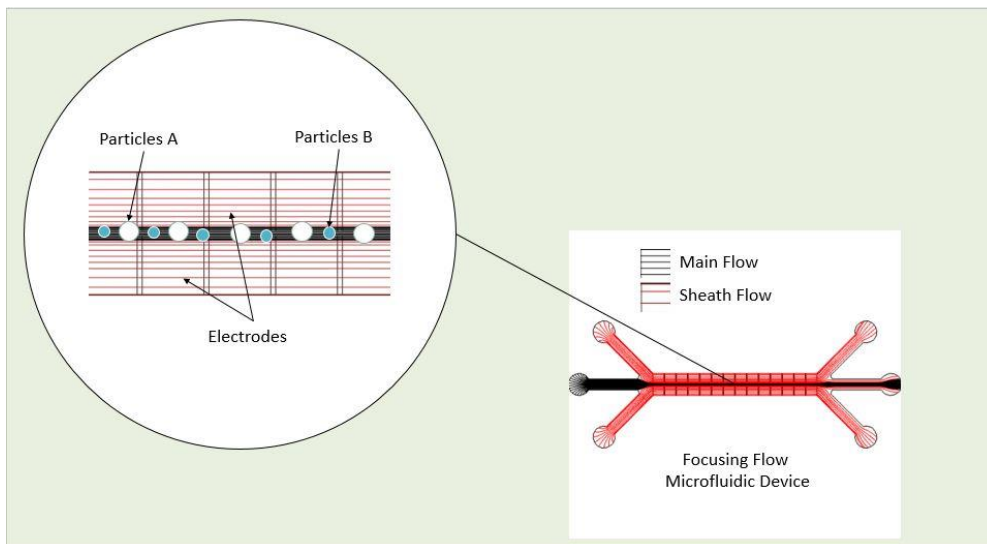


**Figure 3 (b).** Particles flow in Flow Focusing Microfluidic Device.

## 2. MATERIAL AND METHODS

### 2.1 Microfluidics Design

We use 3D CAD software (SolidWorks2020) to design our channel. Schematic diagram of the proposed design is shown in Figure 4. The flow-focusing microfluidic device consists of three inlets and three outlets. The two side inlets are used as sheath flow, while the middle inlet is used for the main flow. Therefore there are three flow streams in the channel. By adjusting the flow rate of the main flow, we can tune the width of the main stream to the centre of the electrodes.

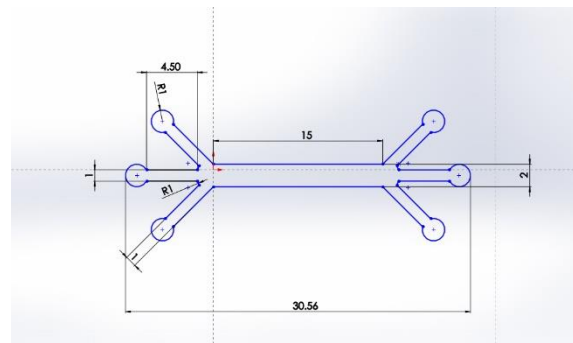


**Figure 4.** Microchannel Design in millimetre-scale.

## 2.2 Flow Simulation

To predict the width of the flow focusing, a numerical simulation study has been done using Comsol Multiphysics 5.4. A theoretical volumetric flow rate ratio was studied to obtain the desired width of the flow focusing. The simulation was a model under the conditions of a laminar flow and time stationary using a 2D model. In this model, we use a constant flow rate for sheath flow, which is  $500\mu\text{l}/\text{m}$  while manipulating the main sample flow rate, which is 100, 300, and  $500\mu\text{l}/\text{m}$ . Figure 5 shows the width of the flow focusing with different main sample flow rate. As we can see from Figure 5, the optimum main sample flow rate to minimize the width of the flow focusing towards the centre of the electrodes was a 5:1 ratio between the sheath flow rate and the main flow rate.

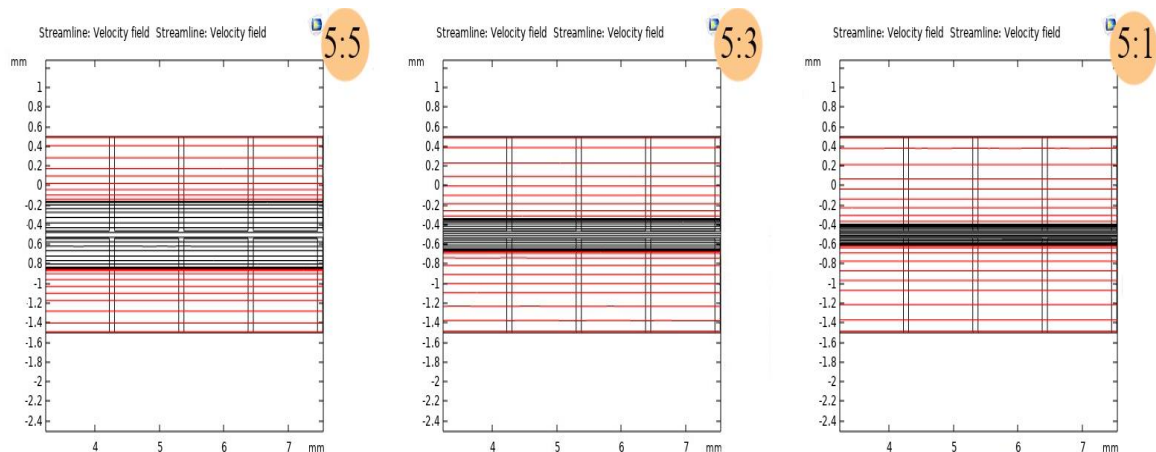


**Figure 5.** Width of the flow focusing at a different flow rate ratio.

## 2.3 Fabrication of Microfluidic Device

The technique utilized for this fabrication process is a soft lithography technique. The process involves a casting process of a polymer material onto a mould. The parts are cast separately, therefore, involve an assembly process. This assembly process involves an alignment and stacking process. The parts are joined together with a bonding technique. Mould design is shown in Figure 6. The depth of the channel is  $500\mu\text{m}$ .

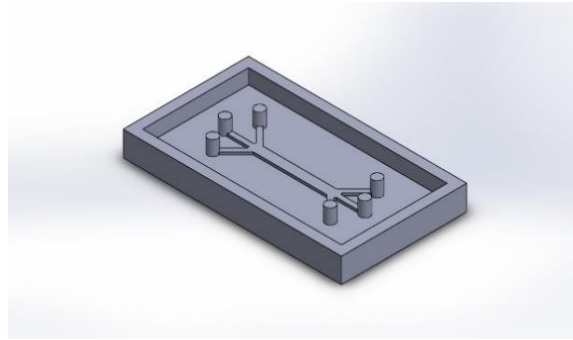


**Figure 6.** Mould Design.

In this experiment, PMMA material was selected because of the cheap and accessible to micro-engraving the features onto the surface. Once the mould is designed, it is then transferred to the software, which is used for the micro-milling machine. The PDMS layer consists of a microchannel that holds the liquid sample and permits the transfer from the inlet to the outlet while the glass slide layer is a substrate that prevents fluid leaking from the channel. We use PDMS as a fluidic layer because of its transparency. Sylgard 184 Silicone Elastomer Base and Curing Agent from Dow Corning Corporation (Midland, MI) are used to produce PDMS. The PDMS base and curing agent were mixed in a ratio of 10:1 by mass and poured into the mould. After that, the fluidics layer and glass slide substrate are bonded using oxygen plasma. We exposed the fluidics layer 50 watts for 5 minutes to give excellent adhesion between those two layers. The process of casting and bonding illustrated in Figure 7.

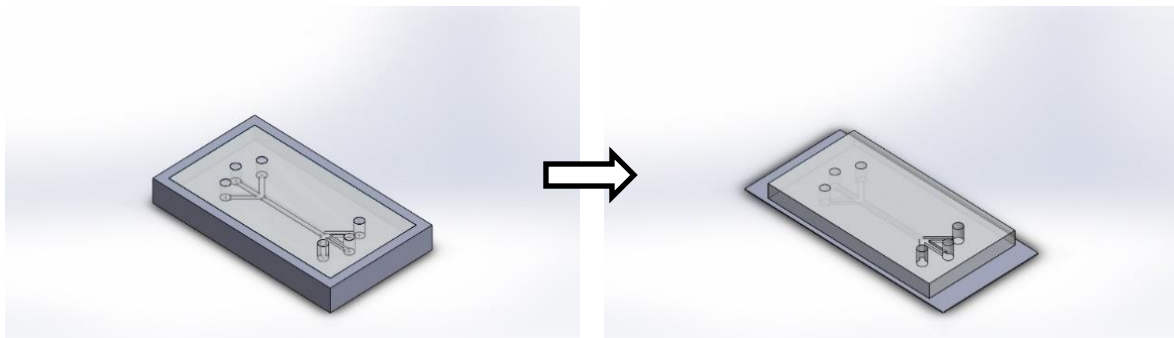


**Figure 7.** PDMS is poured in the mould and cured then removed from the mould and bonded to the glass slide using an oxygen plasma bonding process.

### 3. RESULTS AND DISCUSSION

The fabricated microfluidic device was connected to the Terumo syringe (Tuberculin, 1ml) and syringe pump system (Longerpump, TS-2A/L0107-2A). Microfluidic tubings (Tygon Tube) were inserted into three inlets and one outlet (middle outlet) for the pumping process. Both side outlets are clogged to allow only one pathway exit for fluid flow. The setups are shown in Figure 8. A camera was employed on the top of the device for capturing images and videos during the test.

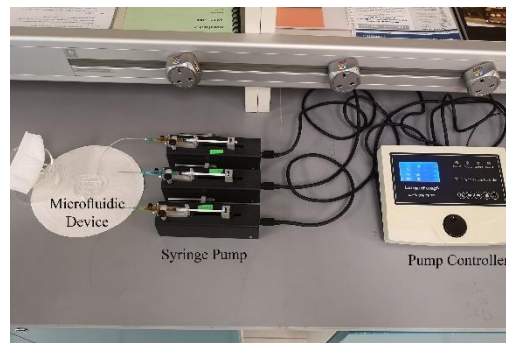


**Figure 8.** Full experimental setup.

### 3.1 Leaking Test

To evaluate the functionality of the fabricated device, a leaking test was conducted. In this investigation, the fluid flow was observed with the same flow rate to observe if there any leaking within the microfluidic channel. We also observe the conditioning fluid flow either its flow in laminar or turbulence. We set up two flow conditions, (a) one inlet one outlet and (b) two inlets one outlet as in Figure 9. The inlets and outlet not been used will be clogged. The flow rate in this experiment is  $500\mu\text{l}/\text{m}$ . Based on Figure 9, we can clearly observe that fluid flow in both conditions was smooth, which means that there is no blockage in the microchannel and leaking between the PDMS layer and a glass slide. Based on the observation from Figure 9 (a), at  $t=0$ , fluid starts to flow from the inlet and continues to flow to the main microchannel at  $t=2\text{s}$ , then reach outlet at  $t=6\text{s}$ . While from Figure 9 (b), at  $t=0$ , both fluid start to flow from the inlet, and both fluid reach at the main microchannel at  $t=1\text{s}$ . Both fluid dominate equal area, and no mixing occur at this phase. This show at the moment both fluid flow under the laminar region. At  $t=3\text{s}$ , bot fluid reaches the outlet.

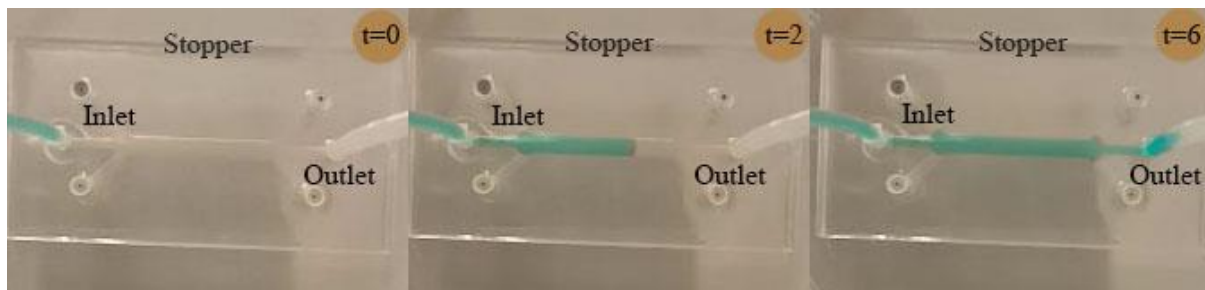


**Figure 9 (a).** Fluid flow one inlet one outlet.

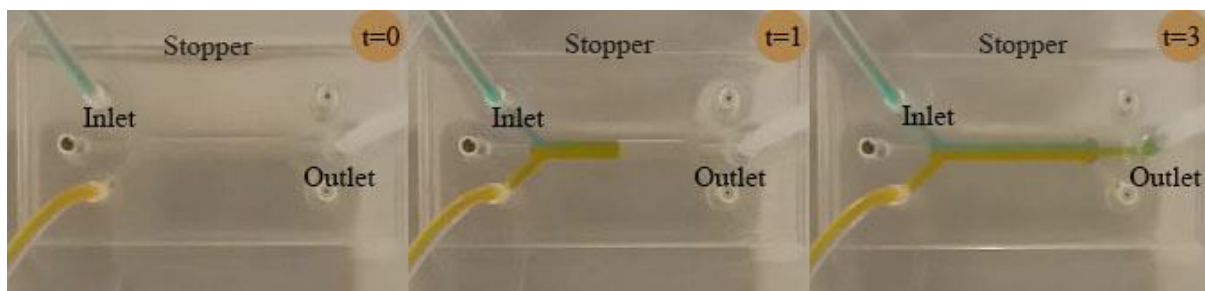


**Figure 9 (b).** Fluid flow two inlets one outlet.

### 3.2 Hydrodynamic Flow Focusing

To visualize and characterize the ability of hydrodynamic flow focusing, two ink solution was used—yellow coloured water used as sheath fluid while blue coloured water used for sample fluid. The fluid is pumped into the system through the inlets. For sheath fluid, the constant flow rate of  $500\mu\text{l}/\text{m}$  is pumped to the channel while the fluid sample flow rate is manipulated at 100, 300, and  $500\mu\text{l}/\text{m}$ . Experimental validation of focusing performance was conducted via monitoring top view of the flow pattern inside the microchannel. Figure 10 shows the focused flow in three different flow rates for sample fluid in the main microchannel. As Figure 10 shows, the main flow was successfully focused in the centre of the main microchannel, all along this channel. From the observation, as the main flow rate ratio to the sheath flow decreasing, the width of the flow focusing decreasing. This observation confirms our findings when compared to the simulation data from Figure 5. From these results, the proposed system is capable of controlling the width of the main stream by controlling the flow rate ratio between the main flow and sheath flow.

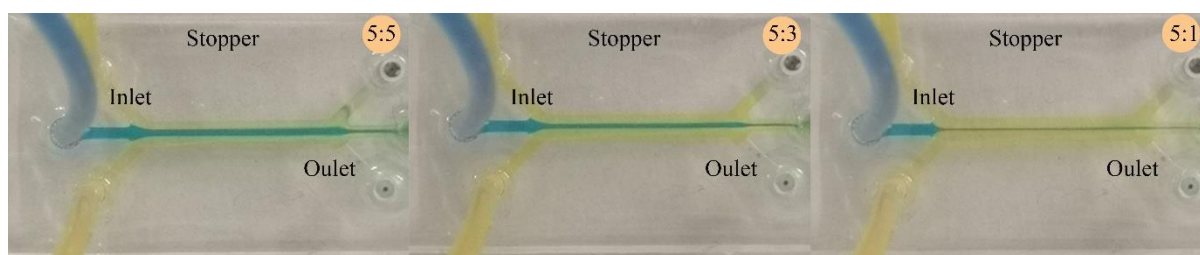


**Figure 10.** Hydrodynamic Flow Focusing at a different main fluid flow rate ratio.

### 4. CONCLUSION

In conclusion, in this paper, we manage to fabricate a hydrodynamic focusing device that can control the width of the main flow by adjusting the flow rate ratio. Our technique relies on our unique microfluidic geometry which performs hydrodynamic focusing, generates flow with three inlets and three outlets. This important feature can turn this device to a potential device for experiments where DEP force involved by integrating with a microelectrode.

### ACKNOWLEDGEMENTS

This research is supported by AKU254: HICOE (FASA2) for Artificial Kidney grant funded by the Ministry of Higher Education (MOHE) Malaysia.

### REFERENCES

- [1] S. Takayama, E. Ostuni, P. LeDuc, K. Naruse, D. E. Ingber, & G. M. Whitesides, "Subcellular positioning of small molecules," *Nature* **411**, 6841 (2001) 1016.
- [2] J. Son, R. Samuel, B. K. Gale, D. T. Carrell, & J. M. Hotaling, "Separation of sperm cells from samples containing high concentrations of white blood cells using a spiral channel," *Biomicrofluidics* **11** (2017) 5.
- [3] C. L. Hansen, E. Skordalakest, J. M. Berger, & S. R. Quake, "A robust and scalable microfluidic metering method that allows protein crystal growth by free interface diffusion," *Proc. Natl. Acad. Sci. U. S. A.* **99**, **26** (2002) 16531–16536.
- [4] A. R. Jafek, S. Harbertson, H. Brady, R. Samuel, & B. K. Gale, "Instrumentation for xPCR Incorporating qPCR and HRMA," *Anal. Chem.* **90**, 12 (2018) 7190–7196.

- [5] A. Bange, H. B. Halsall, & W. R. Heineman, "Microfluidic immunosensor systems," *Biosens. Bioelectron.* **20**, 12 (2005) 2488–2503.
- [6] S. Yan, J. Zhang, D. Yuan, & W. Li, "Hybrid microfluidics combined with active and passive approaches for continuous cell separation," *Electrophoresis* **38**, 2 (2017) 238–249.
- [7] Y. Li, C. Dalton, H. J. Crabtree, G. Nilsson, & K. V. I. S. Kaler, "Continuous dielectrophoretic cell separation microfluidic device," *Lab Chip* **7**, 2 (2007) 239–248.
- [8] M. R. Buyong, F. Larki, M. S. Faiz, A. A. Hamzah, J. Yunas, & B. Y. Majlis, "A tapered aluminium microelectrode array for improvement of dielectrophoresis-based particle manipulation," *Sensors (Switzerland)* **15**, 5 (2015) 10973–10990.
- [9] V. Shkolnikov, D. Xin, & C. H. Chen, "Continuous dielectrophoretic particle separation via isomotive dielectrophoresis with bifurcating stagnation flow," *Electrophoresis* **40**, 22 (2019) 2988–2995.
- [10] S. Täuber, L. Kunze, O. Grauberger, A. Grundmann, & M. Viefhues, "Reaching for the limits in continuous-flow dielectrophoretic DNA analysis," *Analyst* **142**, 24 (2017) 4670–4677.
- [11] M. R. Buyong, A. A. Kayani, A. A. Hamzah, & B. Y. Majlis, "Dielectrophoresis manipulation: Versatile lateral and vertical mechanisms," *Biosensors* **9**, 1 (2019).
- [12] M. R. Buyong, N. A. Aziz, A. A. Hamzah, M. F. M. R. Wee, & B. Y. Majlis, "Finite element modeling of dielectrophoretic microelectrodes based on a array and ratchet type," *IEEE Int. Conf. Semicond. Electron. Proceedings, ICSE*, 3 (2014) 236–239.
- [13] D. Di Carlo, D. Irimia, R. G. Tompkins, & M. Toner, "Continuous inertial focusing , ordering , and separation of particles in microchannels," **104**, 48 (2007).